Supporting Information

Multi-Stimuli Distinct Responsive D-A Based Fluorogen Oligomeric Tool and Efficient Detection of TNT Vapor

Pramod C. Raichure[a], Ramprasad Bhatt[a], Vishal Kachwal[a,b], Tirupati Chander Sharma[c] and Inamur Rahaman Laskar[a]*

[a]*Department of Chemistry, Birla Institute of Technology and Science, Pilani Campus, Pilani, Rajasthan 333031, India.*

[b]*Department of Engineering Science, University of Oxford, Oxford OX1 3PJ, UK.*

[c]*TBRL, DRDO Laboratory, Block D, Sector 30, Chandigarh, India 160003.*

Contents:

14. **Figure S12.** a) Absorption spectrum for pristine P1 (arrow sign shows the band edge absorption), b) The cyclic voltammetry plot of P1 in acetonitrile (ACN) (1 mg P1 in 5 ml ACN); scan rate: 100 mV s^{-1}, c) calculation of HOMO and LUMO energy for P1.
15. **Figure S13.** a) Photograph of emission in P1 film under UV lamp (365 nm); b) absorbance spectrum of P1 film and pristine P1; c) PL intensity spectrum in P1 film (excitation = 397 nm).
16. **Figure S14.** FESEM image of thin film of P1 prepared by drop casting method showing a porous network.
17. **Figure S15.** Photographs of change in the appearance of a dichloromethane (DCM) solution of P1 (1 mg P1 in 10 ml DCM), with a) $BF_3(OEt_2)$, and b) OEt_2 under UV light of 365 nm.
18. **Figure S16.** Plots for change in emission wavelength of a dichloromethane solution of P1 (at excitation 397 nm), a) with each 0.01 ml addition of 12M concentration of hydrochloric acid (HCl), and b) with each 0.01 ml addition of boron trifluoride etherate [$BF_3(OEt_2)$].
19. **Figure S17.** Photographs a) and b) shows the change of emission colour upon 50 μL addition of each of 10M concentrated different protonic acids [hydrochloric acid (HCl), trifluoroacetic acid (TFA), sulfuric acid (H_2SO_4), nitric acid (HNO_3)] were added into the DCM solution of P1 (2 ml solution; 1 mg P1 in 10 ml DCM) under exciting at daylight and UV light (365 nm), respectively, and c) is the photoluminescence (PL) intensity plot for the change in emission (at excitation 397 nm).
20. **Figure S18.** Photographs of a) closed box with lid made from acrylic sheet, b) one glass beaker and powder holder with probe P1 (orange emission under UV lamp of 365 nm) enclosed in a box, c) turned the emission of P1 (red emission under UV lamp of 365 nm) within 10 seconds of contact with vapors generated by acid (1 ml of TFA) filled in the beaker.
21. **Figure S19.** Plots for change in emission wavelength of powder form of P1 (at excitation 397 nm), a) with each minute exposure of trifluoroacetic acid (TFA) vapors, and b) with each minute exposure of boron trifluoride etherate [$BF_3(OEt_2)$] vapors.
22. **Figure S20.** A) Schematic representation of possible interactions of P1 with boron trifluoride etherate $BF_3.[O(CH_2CH_3)_2]$; and B) ^1H NMR spectrum for $CDCl_3$ solution of P1 (5 mg P1 in 0.5 ml $CDCl_3$) and P1+ $BF_3.[O(CH_2CH_3)_2]$ analyzed in $CDCl_3$ solvent.
23. **Figure S21.** Photoluminescence analysis plot for the change in wavelength of P1 (at excitation 397 nm) (i.e., blue-shifted) upon the grinding with time.
24. **Figure S22.** PXRD plot for P1 pristine and P1 ground samples.
25. **Figure S23.** a) It shows the comparative photographs of emission in dilute THF solution of P1 (A) and aggregated compound of P1 in THF-water (B)., b) It shows the comparative emission intensity of the solutions as described (λ_{exc}, 397 nm).

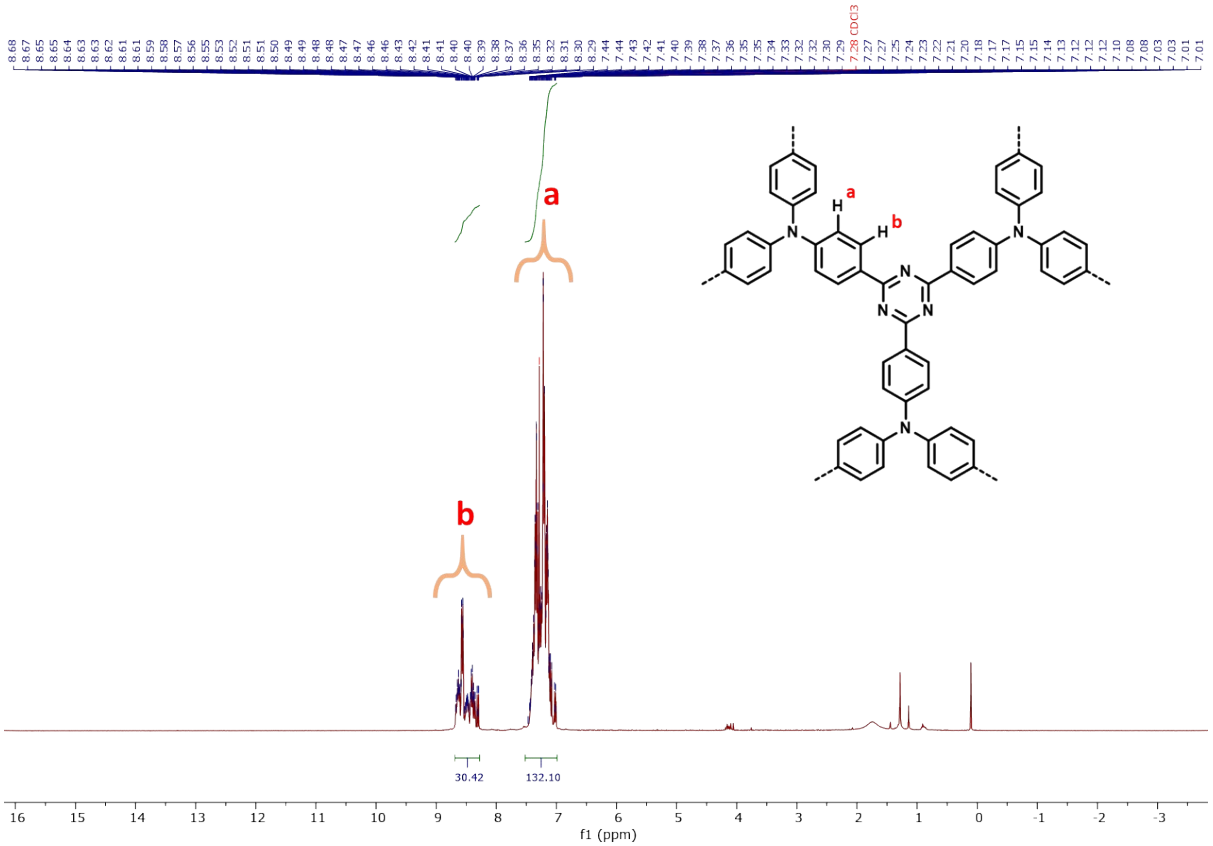

Figure S1. ^{1}H NMR spectrum of P1 recorded in $CDCl_3$ solvent.

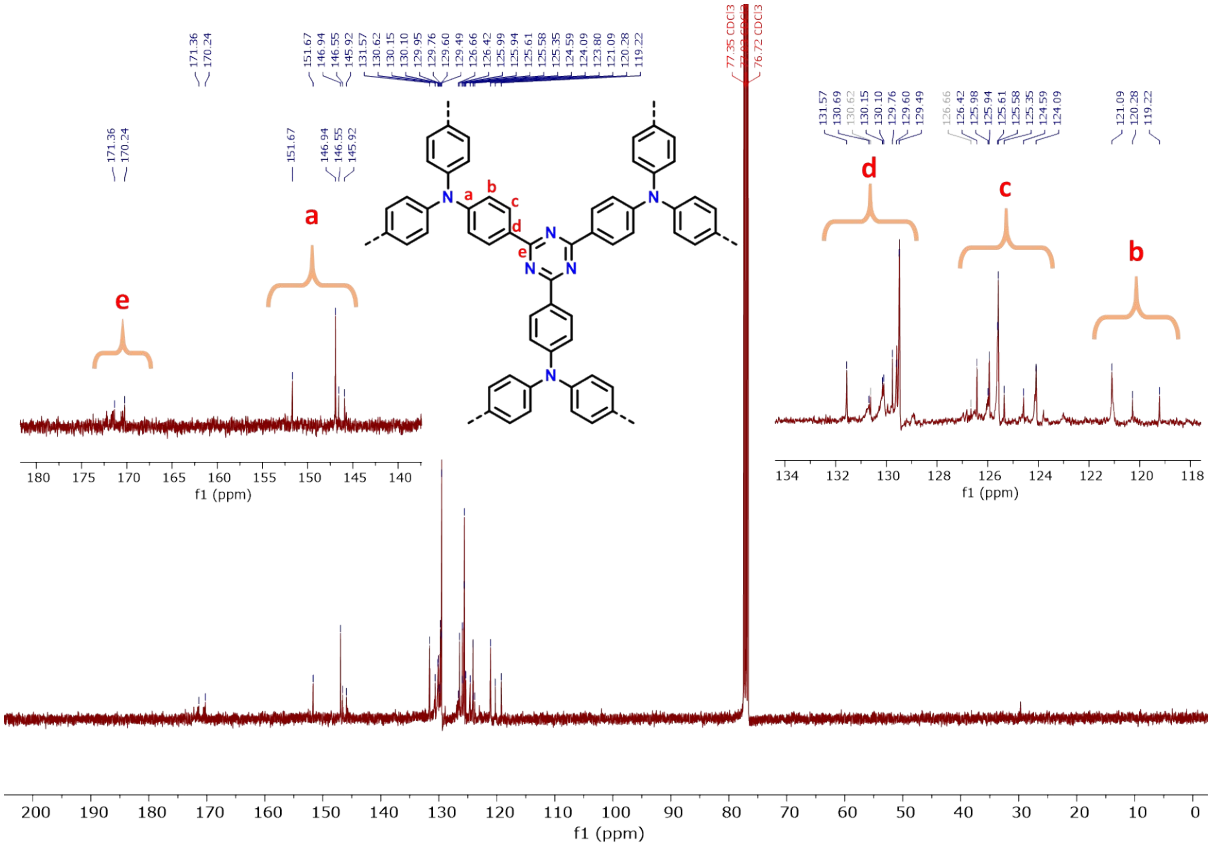

Figure S2. ^{13}C NMR spectrum of P1 recorded in $CDCl_3$ solvent.

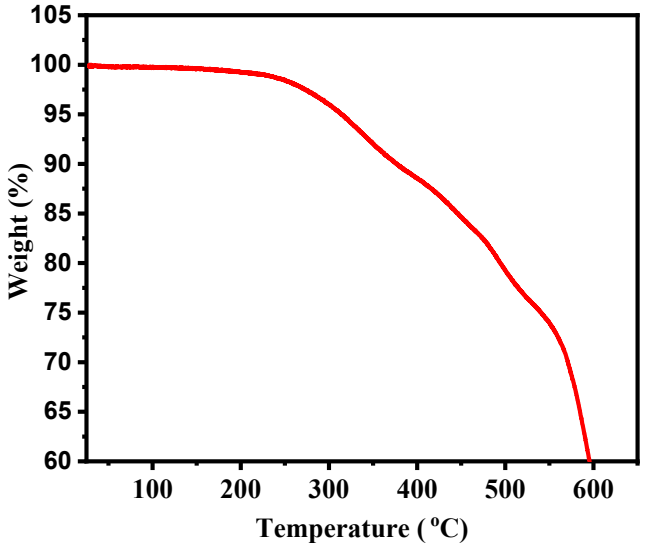

Figure S3. Thermogravimetric analysis (TGA) plot for P1

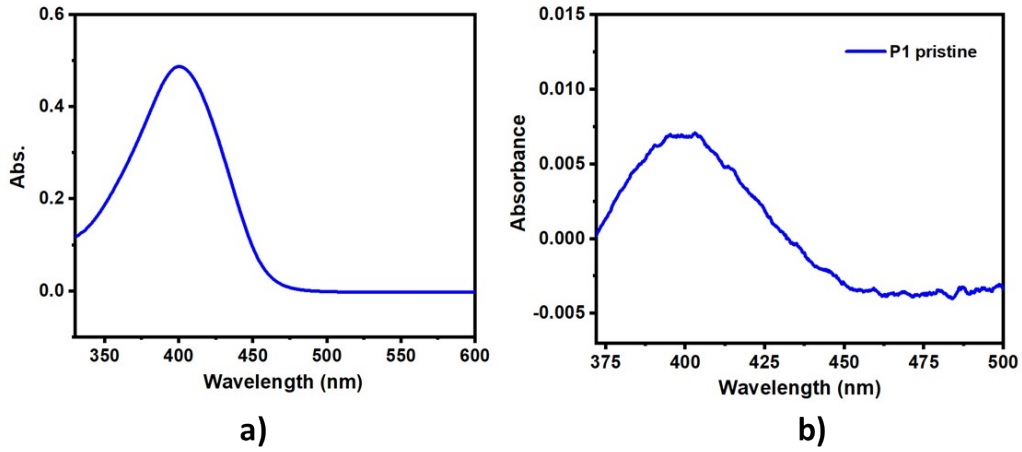

Figure S4. Plots of absorbance in a) THF solution of P1 (1 mg P1 in 50 ml THF) (λ_{abs} = 400 nm), b) P1 pristine (powder/solid form) (λ_{abs} = 400 nm) in absorption mode.

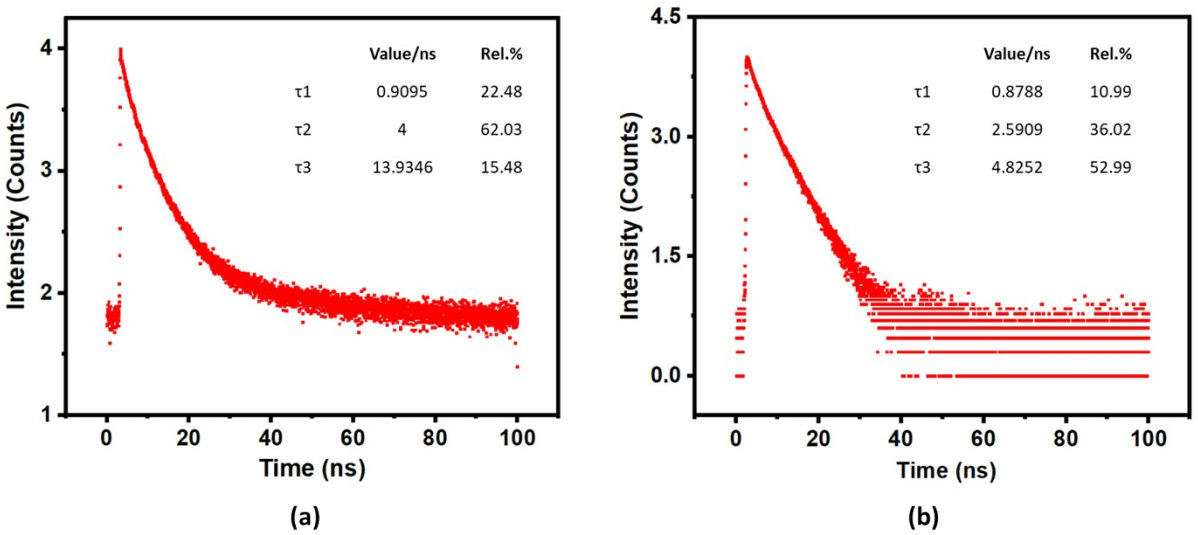

Figure S5. The characteristic fluorescence lifetime decay curve [plot: time (ns) vs intensity that is in, $\log_{10}$ (counts)]: a) for P1 in solid state ($\chi^2 = 1.2$), and b) for THF solution of P1 ($\chi^2 = 1.1$).

Table S1.

The absorption and emission maxima of P1 in different solvents along with Stokes shift and orientation polarisability.

Solvents	Abs. wavelength $\lambda_{max.}$ (nm)	Emission wavelength $\lambda_{max.}$ (nm)	Absorption (cm^{-1})	Emission (cm^{-1})	Stokes shift (cm^{-1})	Orientation polarizability (Δf)
Hexane	396	446	25252.5	22421.5	2831	0.002
Cyclohexane	400	467	25000	21413	3586.7	-0.001
CCl_4	404	478	24752.4	20920.5	3831.9	0.008
Toluene	405	491	24691.3	20366.5	4324.7	0.013
Diethyl Ether	401	496	24937.6	20161.2	4776.3	0.167
Acetone	402	507	24875.6	19723.8	5151.7	0.283
DMF	402	514	24875.6	19455.2	5420.3	0.275
DMSO	404	529	24752.4	18903.5	5848.8	0.265

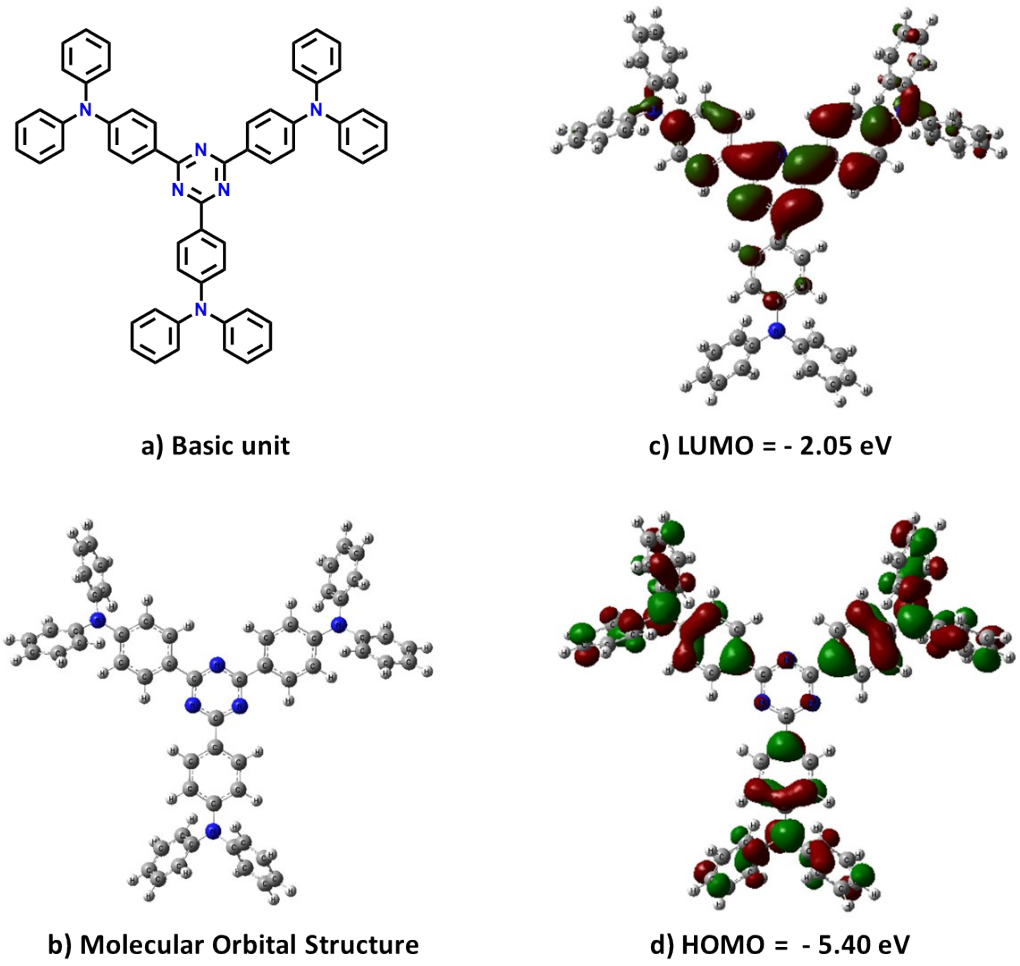

Figure S6. It shows; a) basic unit (the optimized geometry), b) molecular orbital structure, c) HOMO molecular orbitals and d) LUMO molecular orbitals by DFT-based calculation *via* Gaussian 09 at the B3LYP/6-31G.

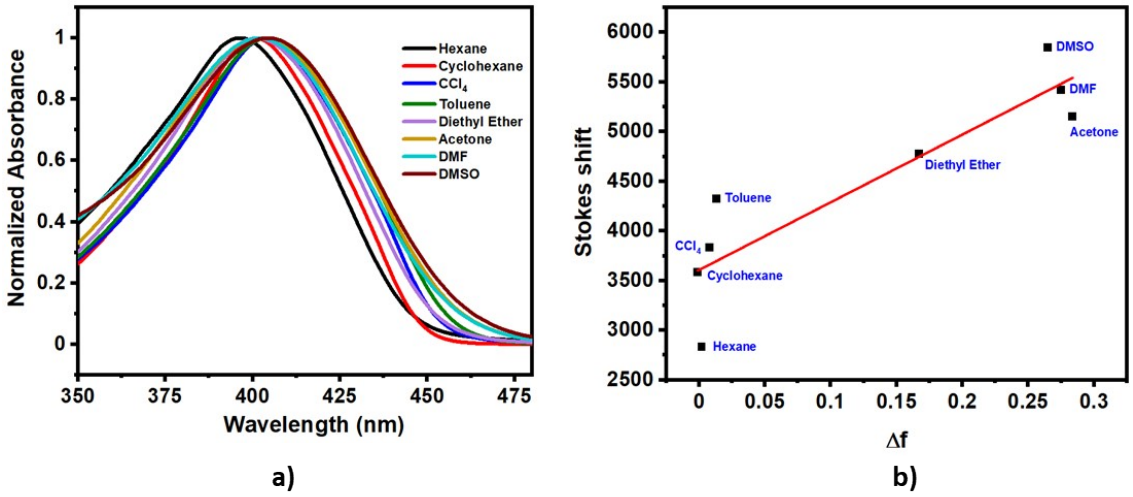

Figure S7. a) Plot of normalized absorbance of P1 with various solvents (1 mg P1 in 10 ml solvent) - hexane, cyclohexane, carbon tetrachloride (CCl_4), toluene, diethyl ether (D. Ether),

acetone, N, N-dimethylformamide (DMF), dimethyl sulfoxide (DMSO); b) Plot of Stokes shift *vs.* orientation polarizability (Δf) shows an approximate linear variation in Stokes shift with polarity of the solvents.

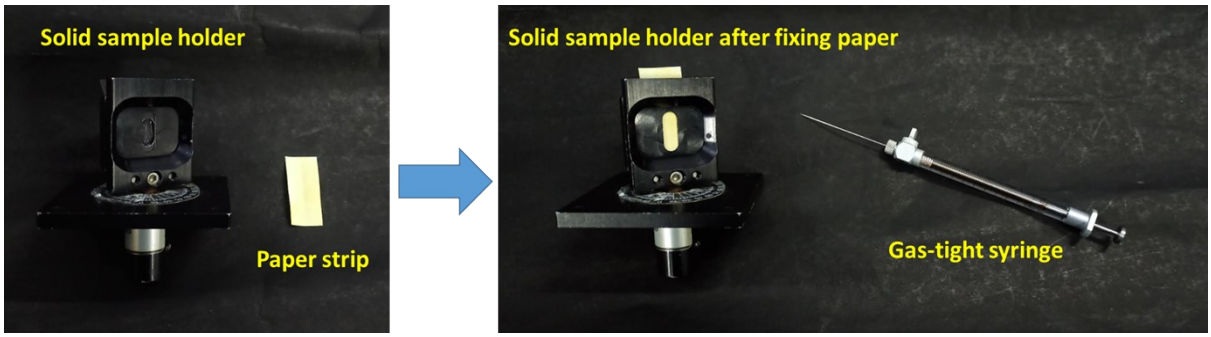

Figure S8. Set-up used for TNT vapor detection: solid sample holder, P1 impregnated filter paper strip, gas-tight syringe.

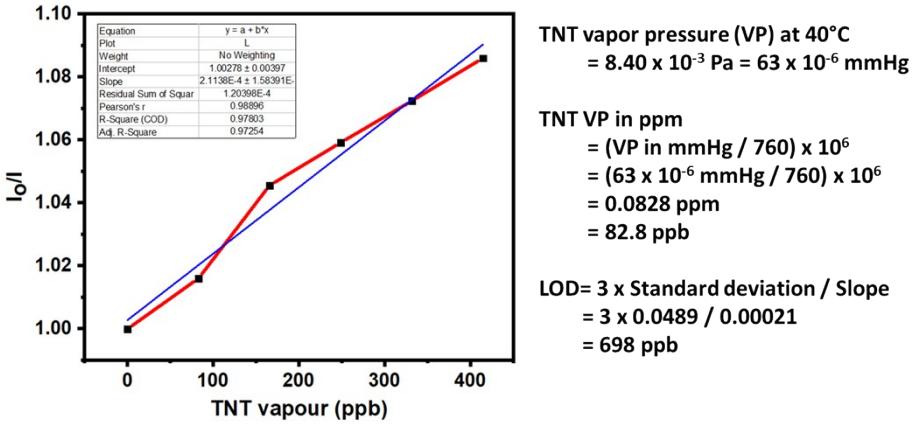

Figure S9. a) Stern–Volmer plots for TNT vapor exposure (Pearson's r value= 0.98); b) calculation of limit of detection (LOD) for P1 with TNT vapor.

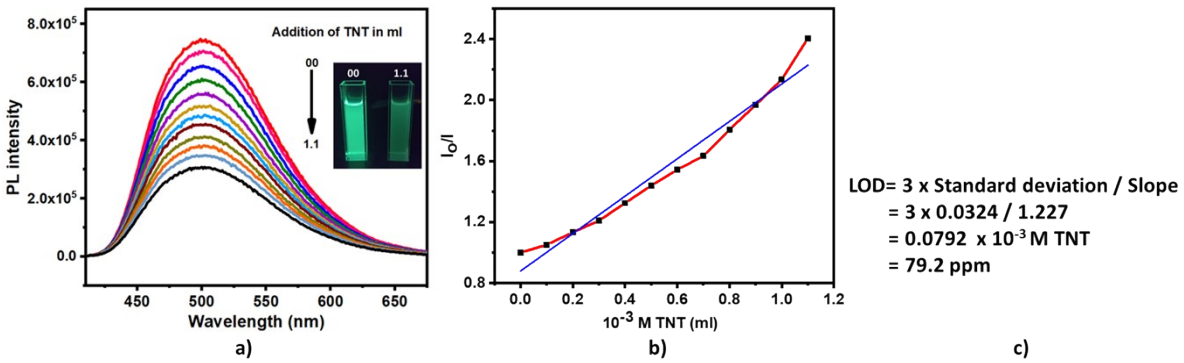

Figure S10. a) PL intensity plot for fluorescence emission quenching after each addition of 0.1 ml solution of aq. TNT (10^{-3}M) to P1 in THF (1 mg P1 in 10 ml THF) (excitation =397 nm); b) the corresponding Stern-Volmer plot; c) calculation of limit of detection (LOD) for P1 with TNT solution.

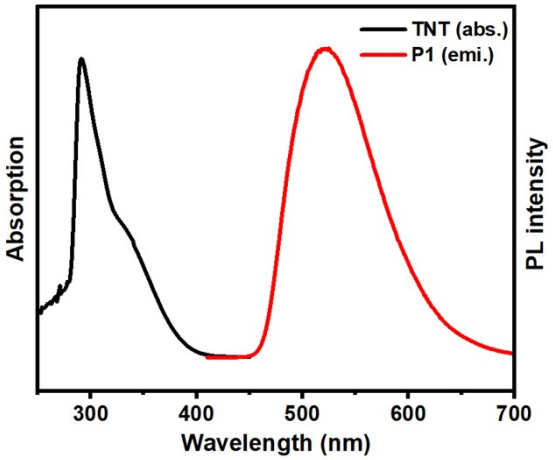

Figure S11. Absorption and emission spectra of solution of TNT and P1 (in THF): black = TNT (absorption) and red = P1 (emission observed under the 360 nm excitation).

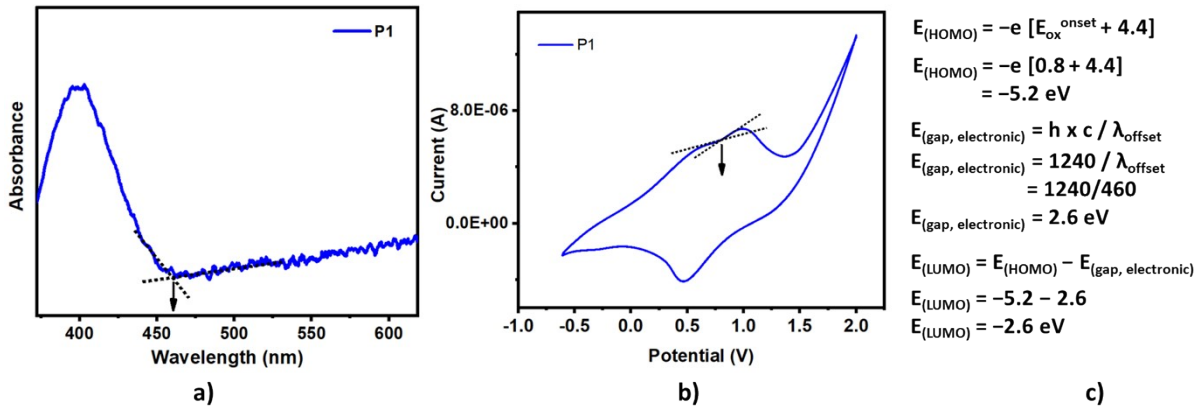

Figure S12. a) Absorption spectrum for pristine P1 (arrow sign shows the band edge absorption), b) The cyclic voltammetry plot of P1 in acetonitrile (ACN) (1 mg P1 in 5 ml ACN); scan rate: 100 mV s^{-1}, c) calculation of HOMO and LUMO energy for P1.

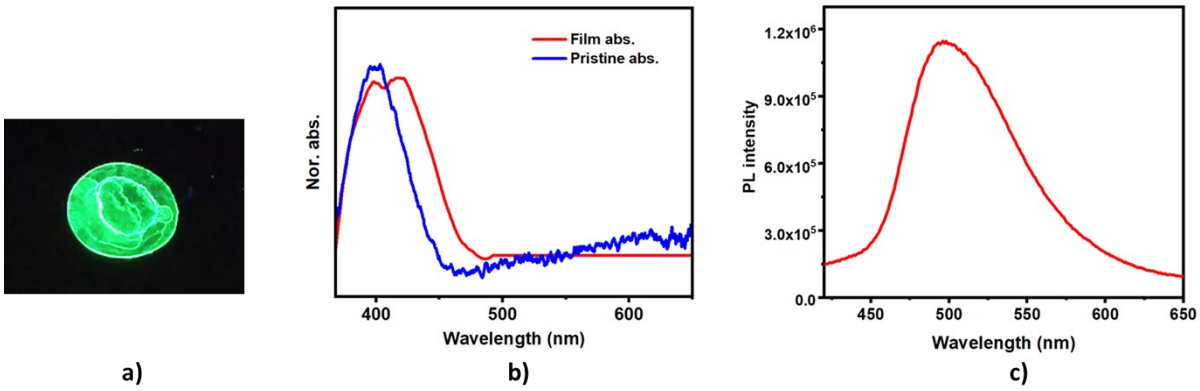

Figure S13. a) Photograph of emission in P1 film under UV lamp (365 nm); b) absorbance spectrum of P1 film and pristine P1; c) PL intensity spectrum in P1 film (excitation = 397 nm).

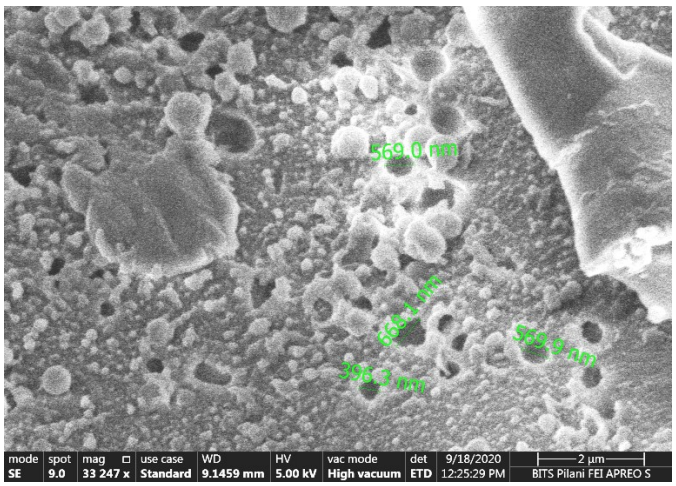

Figure S14. FESEM image of thin film of P1 prepared by drop casting method showing a porous network.

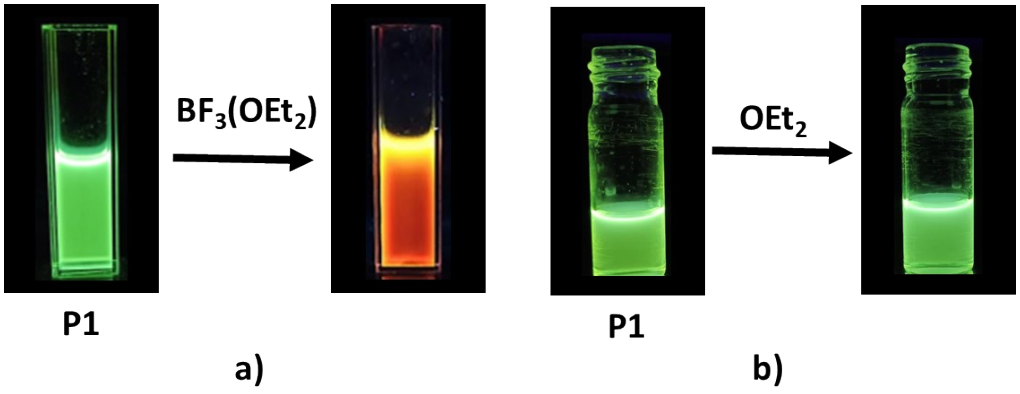

Figure S15. Photographs of change in the appearance of a dichloromethane (DCM) solution of P1 (1 mg P1 in 10 ml DCM), a) with $BF_3(OEt_2)$ (0.4 ml), and b) with OEt_2 (0.4 ml) under UV light of 365 nm.

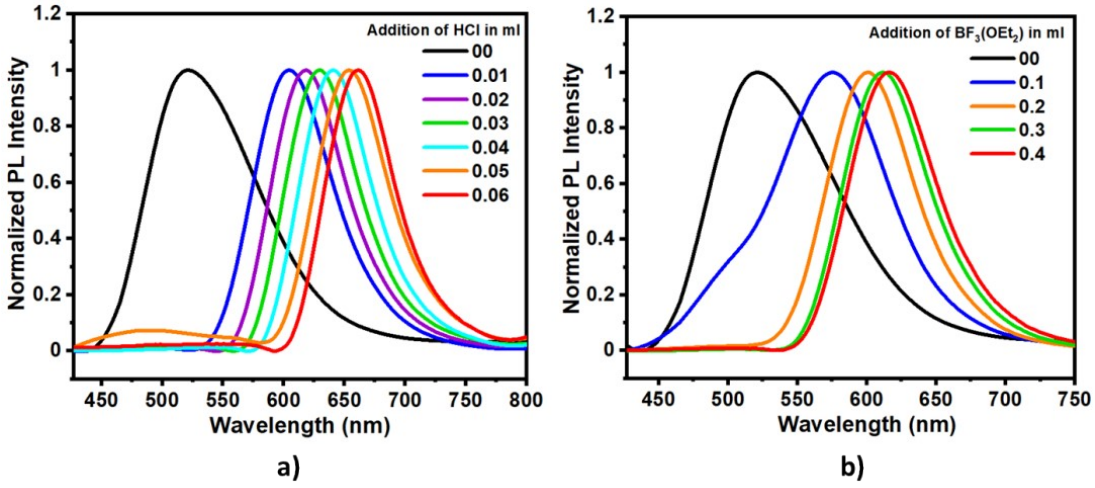

Figure S16. Plots for change in emission wavelength of a dichloromethane solution of P1 (at excitation 397 nm), a) with each 0.01 ml addition of 12M concentrated hydrochloric acid (HCl), and b) with each 0.1 ml addition of boron trifluoride etherate [$BF_3(OEt_2)$].

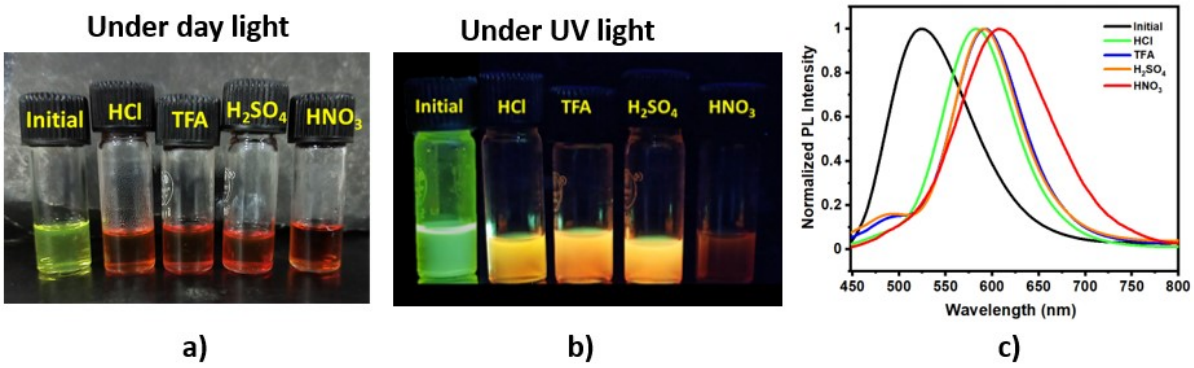

Figure S17. Photographs a) and b) shows the change of emission colour upon 50 µL addition of each of 10M concentrated different protonic acids [hydrochloric acid (HCl), trifluoroacetic acid (TFA), sulfuric acid (H_2SO_4), nitric acid (HNO_3)] were added into the DCM solution of P1 (2ml solution; 1mg P1 in 10ml DCM) under daylight and UV light (365 nm), respectively, and c) is the photoluminescence (PL) intensity plot for the change in emission (at excitation 397 nm).

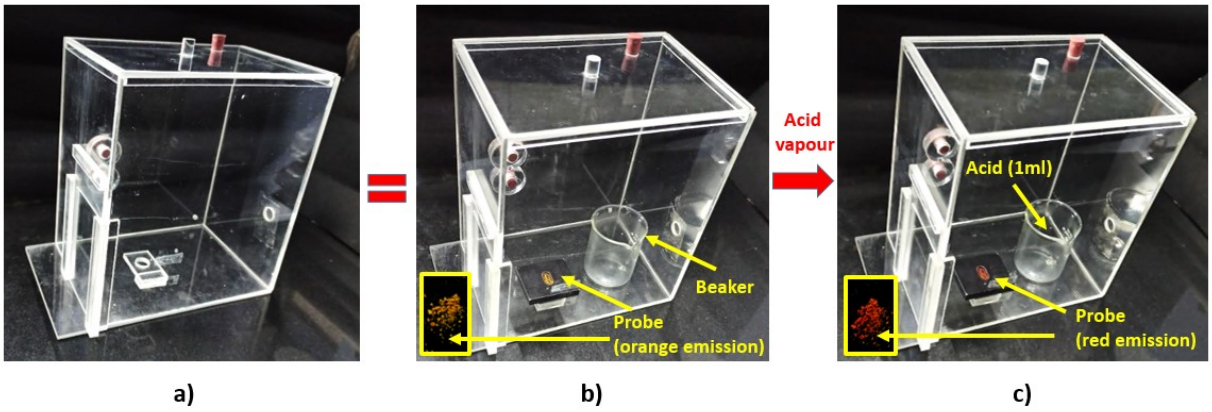

Figure S18. Photographs of a) closed box with lid made from acrylic sheet, b) one glass beaker and powder holder with probe P1 (orange emission excited by UV lamp at 365 nm) enclosed inside the box, c) turned the emission of P1 (red emission excited by UV lamp at 365 nm) within 10 seconds of contact with vapors generated by acid (1 ml of TFA) filled in the beaker.

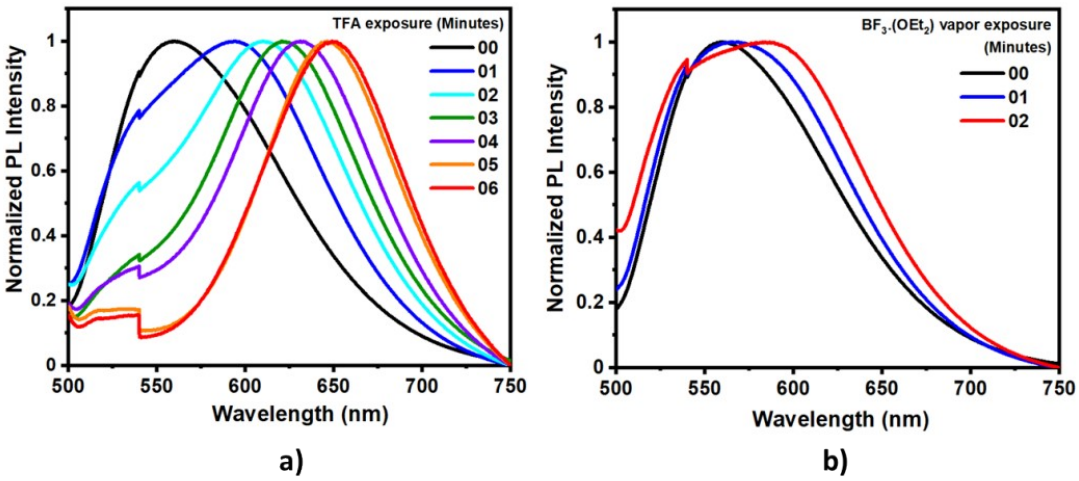

Figure S19. Plots for change in emission wavelength of powder form of P1 (at excitation 397 nm), a) with each minute exposure of trifluoroacetic acid (TFA) vapors, and b) with each minute exposure of boron trifluoride etherate [$BF_3(OEt_2)$] vapors.

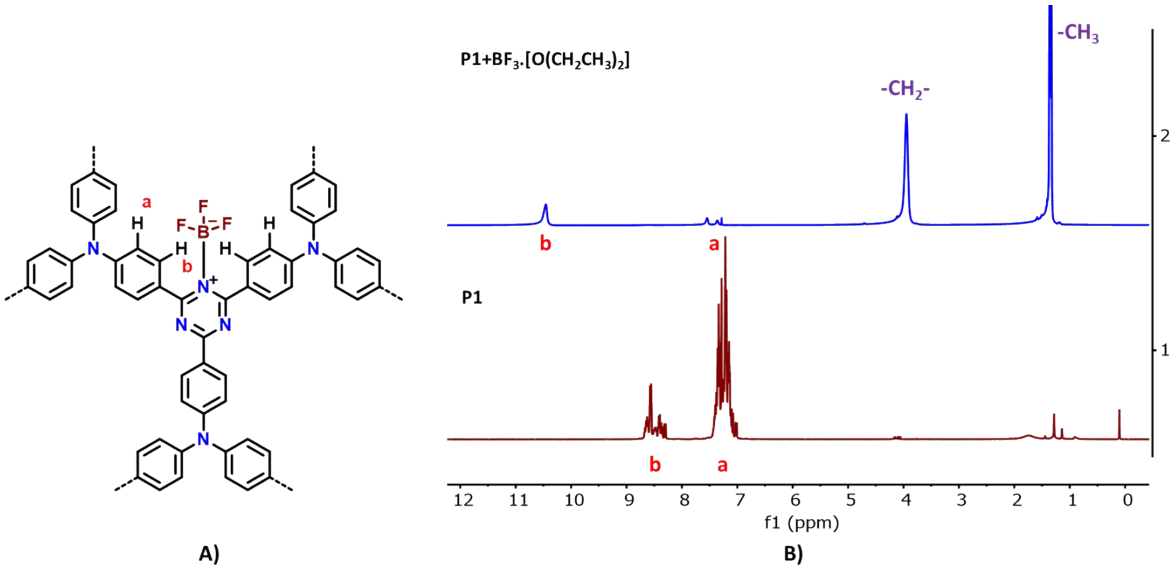

Figure S20. A) Schematic representation of possible interactions of P1 with boron trifluoride etherate $BF_3.[O(CH_2CH_3)_2]$; and B) ^1H NMR spectrum for $CDCl_3$ solution of P1 (5 mg P1 in 0.5 ml $CDCl_3$) and P1+ $BF_3.[O(CH_2CH_3)_2]$ analyzed in $CDCl_3$ solvent.

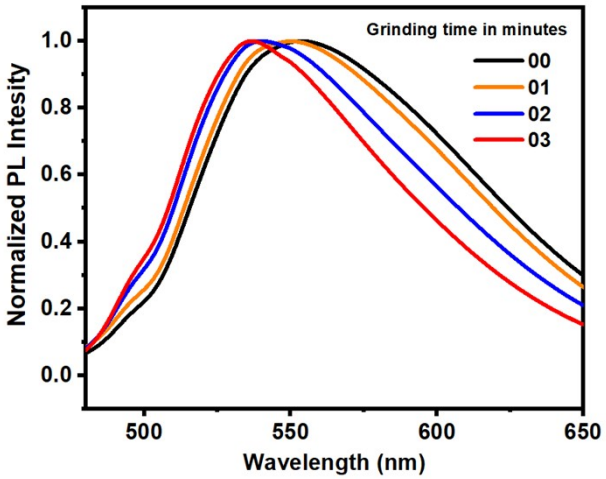

Figure S21. Photoluminescence plot for the change in wavelength of P1 (at excitation 397 nm) (i.e., blue-shifted) upon the grinding with time.

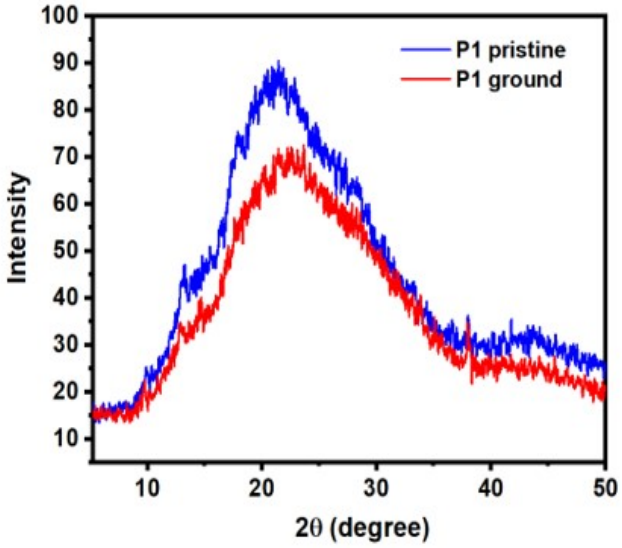

Figure S22. PXRD plot for P1 pristine and P1 ground samples.

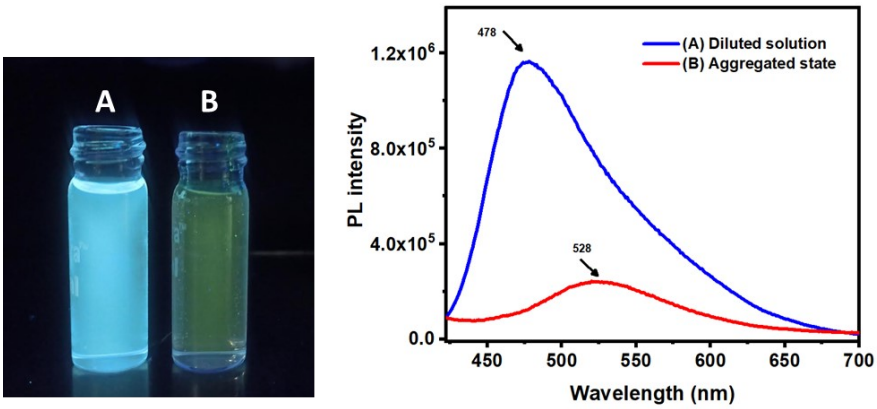

Figure S23. a) It shows the comparative photographs of emission in dilute THF solution of P1 (A) and aggregated compound of P1 in THF-water (B)., b) It shows the comparative emission intensity of the solutions as described (λ_{exc}, 397 nm).

The solutions under a) were prepared by following the given method:
Here, an equal volume (0.5 ml) of P1 probe solution (1 mg P1 in 5 ml THF) taken in two different glass vials of 5 ml volume (A and B). 'A' vial diluted up to 5 ml by THF (diluted solution state) and 'B' vial make up to 5 ml by addition of water 4.5 ml (90% aggregated) to form aggregated state of P1.